A wedge resolution comparison between RTM and the first migration method that is equally effective at all frequencies at the target: tests and analysis with both conventional and broadband data

Yanglei Zou, Qiang Fu, and Arthur B. Weglein, M-OSRP/Physics Dept./University of Houston

DOI:10.1190/segam2017-17784079.1

SUMMARY

Acquiring lower-frequency seismic data is an industry-wide interest. There are industry reports that (1) when comparing the new and more expensively acquired broad-band lower-frequency data with conventional recorded data, taken over a same region, these two data sets have the expected difference in frequency spectrum and appearance, but (2) they often provide less than the hoped for difference in structural resolution improvement or added benefit for amplitude analysis at the target and reservoir. In Weglein et al. (2016) and Q. Fu et al. (2017), they demonstrate that all current migration and migration-inversion methods make high-resolution asymptotic assumptions. Consequently, in the process of migration, they lose or discount the information in the newly acquired lowest-frequency components in the broadband data. The new Stolt extended Claerbout III migration for heterogeneous media (Weglein et al. 2016) addresses this problem as the first migration method that is equally effective at all frequencies at the target and reservoir. That allows the broadband lower frequency data to provide full benefit for improving structural resolution and amplitude analysis. Q. Fu et al. (2017) provide the first quantification of the difference and impact on resolution for RTM (CII) and Stolt extended CIII. In this paper, we continue to study and quantify these differences in the migration resolution using a wedge model and define the added resolution value provided by the new Stolt extended CIII migration for heterogeneous medium. The side lobes of the images of upper and lower reflectors produce an interference that determines resolution. The migration method with a greater reduction of side lobes will be the migration with a greater ability to resolve two reflectors with a same bandwidth in the data, conventional or band limited.

INTRODUCTION

Migration methods that use wave theory for seismic imaging have two components: (1) a wave-propagation concept and (2) an imaging condition. Today all migration methods make a high-frequency approximation in (1) or (2) or both (1) and (2). Our new migration method, Stolt extended CIII for heterogeneous media is the first migration method that makes no high-frequency approximation in both components (1) and (2), for a heterogeneous medium, and is equally effective at all frequencies at the target and/or the reservoir. Weglein (2016) provides a detailed development of this new migration method.

For the imaging principle component, a good start is Jon Claerbout's 1971 landmark contribution (Claerbout, 1971) where three imaging principles are described. The first is the exploding-reflector model for stacked or zero-offset data, which we call Claerbout imaging principle I (CI). The second is time-space coincidence of upgoing and downgoing waves, which we call Claerbout imaging principle II (CII). Waves propagate down from the source, are incident on the reflector, and the reflector generates a reflected upgoing wave. According to CII, the reflector exists at the location in space where the wave that is downward propagating from the source and the upwave from the reflector are at the same time and space. All RTM methods are based on RTM (CII) imaging principle and we after refer to RTM in this paper as RTM (CII). The third is Claerbout imaging principle III (CIII), which starts with surface source and receiver data and predicts what a source and receiver would record inside the earth. CIII then arranges the predicted source and receiver to be coincident and asks for $t = 0$. If the predicted coincident source and receiver experiment at depth is proximal to a reflector one gets a non-zero result at time equals zero. Stolt and his colleagues provided several major extensions of CIII and we refer to that category of imaging principles/methods as Stolt extended CIII.

RTM (CII) and Stolt extended CIII are of central industry interest today, since we currently process pre-stacked data. RTM (CII) and Stolt extended CIII will produce different results for a separated source and receiver located in a homogeneous half space above a single horizontal reflector. That difference forms a central and key message of this paper.

CII can be expressed in the form

$$I(\vec{x}) = \sum_{\vec{x}_s} \sum_{\omega} S'(\vec{x}_s, \vec{x}, \omega) R(\vec{x}_s, \vec{x}, \omega), \tag{1}$$

where R is the reflection data (for a shot record), run backwards, and S' is the complex conjugate of the source wavefield.

A realization of CIII is Stolt FK migration (Stolt, 1978)

$$\begin{aligned} M^{stolt}(x,z) = & \frac{1}{(2\pi)^3} \iiint d\omega dx_g dx_s dk_{sx} \\ & \times \exp(-i(k_{sz}z + k_{sx}(x - x_s))) \\ & \times \int dk_{gx} \exp(-i(k_{gz}z + k_{gx}(x - x_s))) \\ & \times \int dt \exp(i\omega t) D(x_g, x_s, t). \end{aligned} \tag{2}$$

The weighted sum of recorded data, summed over receivers, basically predicts the receiver experiment at depth, for a source on the surface. The sum over sources predicts the source in the subsurface. Then the predicted source and receiver experiment is output for a coincident source and receiver, and at time equals zero; it defines a Stolt extended CIII image. Each step (integral) in this Stolt extended CIII has a specific physically interpretable purpose towards the Stolt extended CIII image.

RTM IS A HIGH-FREQUENCY APPROXIMATION

Today all migration methods assume a high-frequency approximation in a wave-propagation concept or an imaging condition or both. How does one know if a migration method has made a high-frequency approximation? If you have a ray-based travel time picture of candidate images in the migration process at any step or stage in the migration method, then the migration method has made an asymptotic high-frequency assumption/approximation. As we will see for RTM (CII), for one source and one receiver, the image is an ellipse. If you have a travel-time ellipse of candidate images, that is an absolute indicator that the migration method has made a high-frequency approximation.

In Figure 2 and 3, we compare the results of RTM (CII) and Stolt extended CIII for one source and one receiver, RTM (CII) provides an ellipse while Stolt extended CIII does not. Stolt extended CIII provides a local image. For RTM (CII), in this simplest case, where the data is perfect and the medium is homogeneous, the contribution from one source and one receiver, you obtain a set of candidates. Stolt extended CIII will never provide candidates. Stolt extended CIII will bring you to a point in the earth where you have a coincident source and receiver experiment. At time equals zero, if there is a non zero result, you are at a reflector. There is structure there, not a possible or candidate structure. The result from RTM (CII) is a set of candidates of possible structure. That is intrinsic to CII, hence intrinsic to all current RTM. Hence, if you are imaging with RTM or any extension of RTM, it is worth noting that you have made a high-frequency approximation in your migration methods.

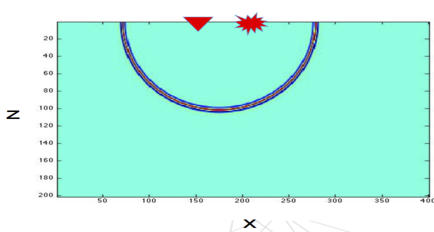

Figure 1: 2D RTM (CII) result for one source and one receiver. High-frequency assumption

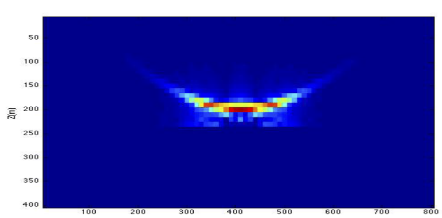

Figure 2: 2D CIII Stolt migration result for one source and one receiver. No high-frequency assumption

All RTM (CII) imaging, i.e., all RTM methods in use today, incorporate high-frequency approximations/assumptions in the imaging principle itself, regardless of how they are implemented. For a heterogeneous medium and assuming one-way propagation (at a point, or overall downgoing between source and reflector and then upgoing from reflector to receiver), a high-frequency approximation has been made, even if you are adopting a CIII imaging principle.

Equation 3 is the new Stolt extended CIII migration method for heterogeneous media of Weglein et al. (2016).

$$P = \int_{S_s} \left[\frac{\partial G_0^{DN}}{\partial z_s} \int_{S_g} \left\{ \frac{\partial G_0^{DN}}{\partial z_g} P + \frac{\partial P}{\partial z_g} G_0^{DN} \right\} dS_g \right. \\ \left. + G_0^{DN} \frac{\partial}{\partial z_s} \int_{S_g} \left\{ \frac{\partial G_0^{DN}}{\partial z_g} P + \frac{\partial P}{\partial z_g} G_0^{DN} \right\} dS_g \right] dS_s \quad (3)$$

Equation 3 was Stolt extended CIII imaging for a heterogeneous medium, and doesn't assume one-way propagation at either a point, or, separately, overall between source and reflector, and, reflector to receiver. G_0^{DN} is the Green's function for the heterogeneous medium that vanishes along with its normal derivative at the lower surface of the migration volume (Weglein et al., 2011b). Equation 3 is the first migration method that makes no high-frequency approximation in both wave-propagation concept and in the imaging condition for heterogeneous media, i.e., it is equally effective at all frequencies at the target and at the reservoir. For details please see Weglein et al. (2011a,b) and F. Liu and Weglein (2014).

QUANTIFY THE DIFFERENCE AND IMPACT ON RESOLUTION

To quantify the impact and to examine how different migration methods treat different bandwidths in the data, we examine the relative reduction of side-lobe amplitudes for each migration method using conventional and band-limited data. Side lobes in the data are an expression of the band-limited source. For events in the data, the more we extend the low-frequency content of the spectrum, (1) the smaller the amplitude of side lobes and (2) the closer the side lobes move towards the center of the event.

Fu et al. (2017) produced the first direct comparison of differences in structural resolution produced by RTM (CII) and Stolt extended CIII using data with and without low frequencies and the same homogeneous velocity model. There are two factors that contribute to these differences: (1) the imaging condition itself and (2) the way the imaging condition is implemented. In RTM (CII) both the imaging condition and how the imaging condition is implemented are each separately making high-frequency approximations. In the new imaging method (Stolt extended CIII for heterogeneous media) from M-OSRP both the imaging condition and method of implementation are equally effective at all frequencies at the target and reservoir. There are side lobes in the structural image due to the missing low frequencies. With the new imaging method see equation 3 and including low frequencies in the input data the side lobes are reduced 57% (from 0.33 to 0.14) whereas the conventional leading edge RTM only reduced the side lobes by 21% (from 0.78 to 0.62). The new imaging method equation 3 is able to benefit from broadband data for structural resolution improvement to a much greater extent than the current best industry standard.

In this paper we continue to study the resolution differences of RTM (CII) and Stolt extended CIII. We produce the first wedge-model test for the comparison of structural resolution differences with data with and without low frequencies, using the same homogeneous velocity model, comparing RTM (CII) and Stolt extended CIII. With Stolt extended CIII and including low frequencies in the input data the side lobes are reduced 87% whereas RTM (CII) only reduced the side lobes by 50%. More low frequency was included in these tests than in the earlier Q. Fu et al (2017) tests. This result is consistent with the result in Fu et al. (2017). Stolt extended CIII is able to benefit from broadband data for structural resolution improvement to a much greater extent than the current best industry standard. The wedge model test in this paper further demonstrates that the Stolt extended CIII result has better resolution than the RTM (CII) result due to the smaller side lobes in the image. For Stolt extended CIII broadband data, two reflectors can be identified when the distance between 2 reflectors is greater than 25m, while for RTM (CII) broadband data the distance between 2 reflectors must be greater than 50m. For Stolt extended CIII conventional data, two reflectors can be identified when the distance between 2 reflectors is greater than 50m. while for RTM (CII) conventional data, the distance between 2 reflectors must be greater than 75m.

NUMERICAL TEST ON A WEDGE MODEL

The tests and comparisons in this paper had a broad band data that had a high frequency cut-off but the spectrum was full on the low end. That gave a limit or end-member for the most improvement in resolution for a layer that the new migration equation 3 could produce with broadband data. This analysis and conclusion does not depend on having data down to zero frequency. We generate the two events separately and then combine them together to generate the two-event synthetic data. For each event, a two half-space model is used, the velocity of upper half-space is 1500m/s and the lower one is 2000m/s. For the first events the interface between the two half-space is 1500m. For the second event, the location is varying from 1512.5m to 1275m to mimic the wedge model. The purpose of this procedure is to correctly locate both of the two events in the image space using a homogeneous velocity model.

The two wavelets used in the tests are both band-limited spikes. The frequency range of the first one (broadband) is 0Hz-50Hz and of the other one (conventional) is 20Hz-50Hz. Figure 5 (upper left and upper right) shows the frequency spectra of the two wavelets and figure 5 (lower left and lower right) shows the time domain waveforms.

Fig 6 shows the RTM (CII) and Stolt extended CIII images for one reflector at 1500m with the two different wavelets. The upper left is the Stolt extended CIII image with broadband data, the lower left is the Stolt extended CIII image with conventional data, the upper right is the RTM (CII) image with broadband data, and the lower right is the RTM (CII) image with conventional data. For Stolt extended CIII the side lobes are reduced more than 87%, whereas for RTM (CII) the side lobes

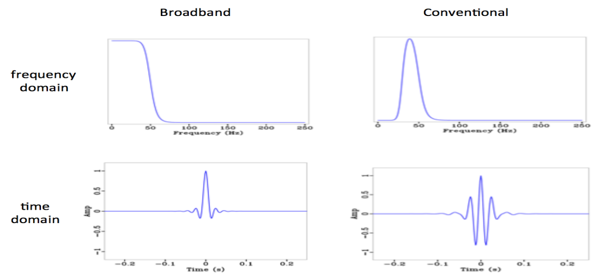

Figure 3: The upper left and upper right show the frequency spectra of the two wavelets; the lower left and lower right show the time-domain waveforms.

reduced only about 50%. This result is consistent with that in Q. Fu et al. (2017).

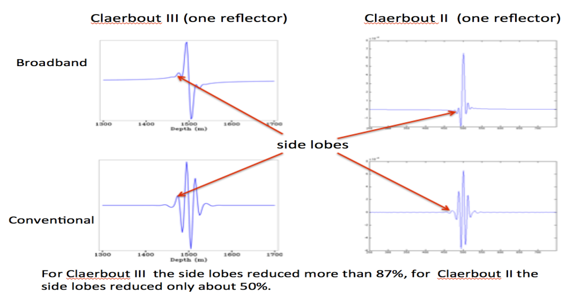

Figure 4: The upper left is the CIII image with broadband data, the lower left is the CIII image with conventional data, the upper right is the RTM (CII) image with broadband data, and the lower right is the RTM (CII) image with conventional data. For CIII the side lobes are reduced more than 87%, whereas for RTM (CII) the side lobes reduced only about 50%. This result is consistent with that in Q. Fu et al. (2017).

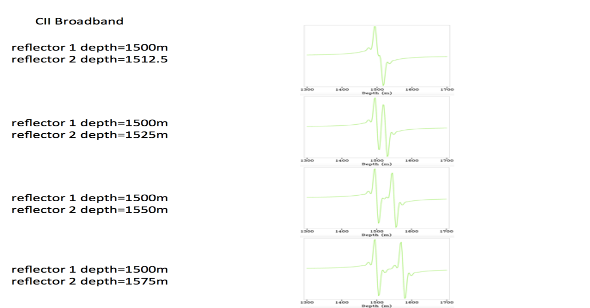

Figure 5: The Stolt extended CIII wedge model image for broadband data with first reflector at 1500m and second reflector at 1512.5m, 1525m, 1550m, 1575m respectively.

Figure 7-10 show the RTM (CII) and Stolt extended CIII image for a wedge model with the broadband data and conventional data. Figure 7 shows the Stolt extended CIII wedge model image for broadband data with the first reflector at 1500m and second reflector at 1512.5m, 1525m, 1550m, 1575m respec-

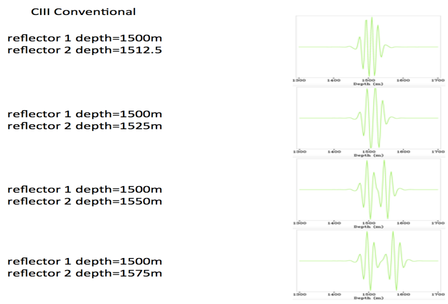

Figure 6: The Stolt extended CIII wedge model image for conventional data with first reflector at 1500m and second reflector at 1512.5m, 1525m, 1550m, 1575m respectively..

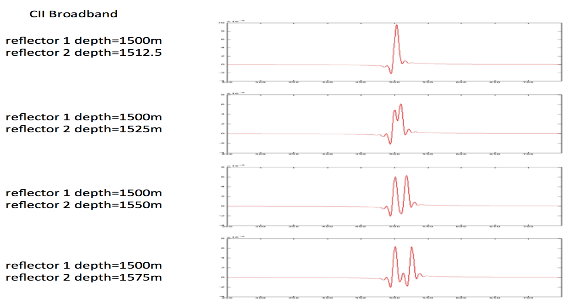

Figure 7: The RTM (CII) wedge model image for broadband data with first reflector at 1500m and second reflector at 1512.5m, 1525m, 1550m, 1575m respectively.

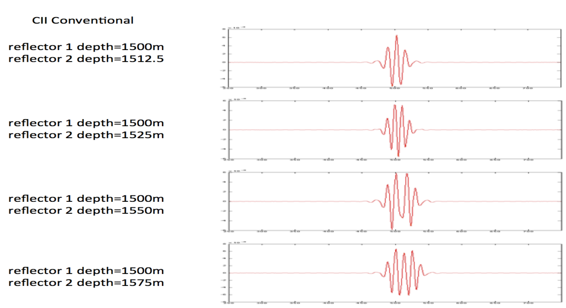

Figure 8: The RTM (CII) wedge model image for conventional data with first reflector at 1500m and second reflector at 1512.5m, 1525m, 1550m, 1575m respectively.

tively. Figure 8 shows Stolt extended CIII wedge model image for conventional data with first reflector at 1500m and second reflector at 1512.5m, 1525m, 1550m, 1575m respectively. Figure 9 shows RTM (CII) wedge model image for broadband data with first reflector at 1500m and second reflector at 1512.5m, 1525m, 1550m, 1575m respectively.Figure 10 shows The RTM (CII) wedge model image for conventional data with first reflector at 1500m and second reflector at 1512.5m, 1525m, 1550m, 1575m respectively.

From the figures we can conclude that two reflectors are separated when the distance between 2 reflectors is greater than 25m for Stolt extended CIII Broadband data, 50m for Stolt extended CIII conventional data, 50m for RTM (CII) Broadband data and 75m for RTM (CII) conventional data.

CONCLUSION

In this paper we produced the first wedge-model test for the comparison of structural resolution differences with data with and without low frequencies, comparing the current leading edge RTM (CII) and the Stolt extended CIII imaging principle. RTM (CII) has a high-frequency assumption in its imaging principle. The Stolt extended CIII imaging principle is not a high-frequency imaging principle. There are side lobes in the structural image due to the missing low frequencies. For a single reflector, including low frequencies in the input data, the side lobes are reduced 87% in Stolt extended CIII whereas the side lobes are only reduced 50% in RTM (CII), which is consistent with the result in Q. Fu et al. (2017). The new imaging method is able to benefit from broadband data for structural resolution improvement to a much greater extent than the current best industry standard migration. The wedge model test in this paper further demonstrates that the Stolt extended CIII result has better resolution than the RTM (CII) result due to the smaller side lobes in the image from each reflector. For Stolt extended CIII with broadband data, two reflectors can be identified when the distance between 2 reflectors is greater than 25m, while for RTM (CII) with broadband data the distance between 2 reflectors must be greater than 50m. For Stolt extended CIII with conventional data, two reflectors can be identified when the distance between 2 reflectors is greater than 50m. While for RTM (CII) with conventional data, the distance between 2 reflectors must be greater than 75m. In this paper we examine the resolution difference for a wedge model. All current migration method (including RTM) assume a one-way propagation model at every point in the subsurface for a smooth velocity model. That one-way propagation model is a high-frequency approximation. The new Stolt extended CIII for heterogeneous media assumes a two-way propagation model at every point in a smoothly varying medium. The next planned tests will include implementation differences (i.e. the wave propagation component of migration) for a smooth velocity model. The differences in resolution derived from the new migration method, Stolt extended CIII for heterogeneous media, that makes no high-frequency approximation in both (A) the wave propagation concept (B) the imaging principle will be greater when both the imaging principle and the wave propagation model are included than we report here for only the imaging principle differences.

ACKNOWLEDGMENTS

We are grateful to all M-OSRP sponsors for encouragement and support in this research. We would like to thank all our coworkers for their help in reviewing this paper and valuable discussions. We would like to thank Dr. Jim Mayhan for his suggestions and help in editing this paper.

EDITED REFERENCES

Note: This reference list is a copyedited version of the reference list submitted by the author. Reference lists for the 2017 SEG Technical Program Expanded Abstracts have been copyedited so that references provided with the online metadata for each paper will achieve a high degree of linking to cited sources that appear on the Web.

REFERENCES

Claerbout, J. F. 1971, Toward a unified theory of reflector mapping: Geophysics, 36, 467–481, http://dx.doi.org/10.1190/1.1440185.

Stolt, R. H. 1978, Migration by Fourier transform: Geophysics, 43, 23–48, http://dx.doi.org/10.1190/1.1440826.

Weglein, A. B. 2016, Multiples: Signal or noise?: Geophysics, 81, V283–V302, http://dx.doi.org/10.1190/geo2014-0486.1.

Weglein, A. B., R. H. Stolt, and J. D. Mayhan 2011a, Reverse time migration and Green's theorem: Part I — The evolution of concepts, and setting the stage for the new RTM method: Journal of Seismic Exploration, 20, 73–90.

Weglein, A. B., R. H. Stolt, and J. D. Mayhan 2011b, Reverse time migration and Green's theorem: Part II — A new and consistent theory that progresses and corrects current RTM concepts and methods: Journal of Seismic Exploration, 20, 135–159.

Weglein, A. B. 2012, Short note: An alternative adaptive subtraction criteria (to energy minimization) for free surface multiple removal. M-OSRP 2011 Annual Report, 375.